POLISH POLAR RESEARCH
vol. 42 no. 1, pp. 1–23, 2021 DOI: 10.24425/ppr.2021.136510

Geodynamic setting of Scotia Sea and its effects on geomorphology of South Sandwich Trench, Southern Ocean

Polina LEMENKOVA

Schmidt Institute of Physics of the Earth, Russian Academy of Sciences.
Bolshaya Gruzinskaya St, 10, Bld. 1, Moscow, 123995, Russian Federation
<pauline.lemenkova@gmail.com>

Abstract: The South Sandwich Trench located eastward of the Drake Passage in the Scotia Sea between Antarctica and South America is one of the least studied deep-sea trenches. Its geomorphological formation and present shape formed under the strong influence of the tectonic plate movements and various aspects of the geological setting, *i.e.*, sediment thickness, faults, fracture zones and geologic lineaments. The aim of this paper is to link the geological and geophysical setting of the Scotia Sea with individual geomorphological features of the South Sandwich Trench in the context of the phenomena of its formation and evolution. Linking several datasets (GEBCO, ETOPO1, EGM96, GlobSed and marine free-air gravity raster grids, geological vector layers) highlights correlations between various factors affecting deep-sea trench formation and development, using the Generic Mapping Tools (GMT) for cartographic mapping. The paper contributes to the regional studies of the submarine geomorphology in the Antarctic region with a technical application of the GMT cartographic scripting toolset.

Keywords: South Atlantic Ocean, Scotia Sea Plate, deep-sea trench, GMT, Geology, Cartography.

Introduction

Rapid development of the computing power, programming languages, and the culture of coding have resulted in rapid advances in machine learning, analysis of big datasets, and automatization of geovisualization. The rise of scripting methods brought about advances in mapping traditionally used by the

Graphical User Interface (GUI), *e.g.*, ArcGIS (Lemenkova 2011; Lemenkova *et al.* 2012; Klaučo *et al.* 2013a, 2013b, 2014, 2017). Scripting and programming languages and tools such as Python, R, Octave, Matlab, and awk allow enhancement of traditional geographical analysis to add advanced level data analysis and plotting to GIS based maps (*e.g.*, Lemenkova 2020d) or perform a statistical plotting in geological data modelling (Agterberg 1964; Davis 1986; Dahlin *et al.* 1999; Lindh 2004). Examples of the advanced geospatial data analysis and visualization are presented in numerous publications on geophysical and gravity modelling (Janik 1997; Grad *et al.* 2002; Yegorova *et al.* 2011; Okoń *et al.* 2016; Pashkevich *et al.* 2018; Tiira *et al.* 2020; Lemenkova 2020e). The Generic Mapping Tools (GMT) presents further steps in the development of traditional cartography, or in the combination of GIS with statistical data analysis, through a combination of both. This makes GMT unique, because it is able to combine cartographic visualization and non-geospatial data analysis and to visualize both vector and raster data using scripts.

Publications on seafloor topography and geomorphology have increased since 1991 with the use of GMT methodology, new datasets and techniques of data capture that visualized the true shape of the ocean seafloor. The bathymetric mapping including both GIS, and multibeam techniques enables to reveal the relief structures hidden beneath kilometers of sea water (Suetova *et al.* 2005; Gauger *et al.* 2007; Schenke and Lemenkova 2008; Leat *et al.* 2010, 2013; Lemenkova 2020a, 2020b, 2020c). However, the South Sandwich Trench is considerably less-well studied than the deep-sea trenches of the Pacific Ocean. This paper aims to contribute to studies of the South Sandwich Trench by analysis of the controls on the geological and geophysical settings affecting its geomorphology.

Caused by the collision and subduction of the tectonic plates and sculptured by the complex interplay of tectonic and sedimentary processes, the geomorphology of oceanic trenches is very complex and diverse. At the same time, their submarine geomorphology is both spectacular in their structural and morphological features and enigmatic due to their remoteness. This necessarily requires special methods of remote sensing data measurements and their processing by advanced GIS tools which enables an automated machine-based digitizing of the series of the cross-sections, necessary to model the geomorphic structure of the trenches. This paper uses several high-resolution datasets for visualizing the geological, tectonic, topographic, and geophysical setting of the Scotia Sea, and processes the grids using the scripting algorithms of the GMT for geomorphological modelling along a set of closely-spaced trench transects.

This paper contributes to studies of ocean trench geomorphology to examine the local settings of the Scotia Sea and South Sandwich Trench in their geological and geophysical contexts, as well as presenting characteristics of the variability in sediment thickness. It mirrors the circulation of bottom water within and between ocean basins, reflects the geological structure and topography of the seafloor and

affects trench geomorphology. The purpose was to visualize the correlation between the geomorphic form and geological evolution of the submarine landforms and to demonstrate how does the functionality of GMT enables to model and map geological and tectonic objects based on the raster grids, to visualize spatially continuous phenomena as three-dimensional datasets: topography, marine free-air gravity anomalies and geoid, geological structures (fracture zones, faults, trench, ridges, large igneous provinces) and spatial distribution of the sediment thickness.

Finally, the paper shown the application of the methods of cartographic automatization aimed at processing of the cross-section profiles for geomorphological modelling, through visualizations of the Scotia Sea basin and geomorphological characterization of the South Sandwich Trench as a set of transects. The visualization of the topographic structure, geodynamics, and geologic composition of the Scotia Sea region and South Sandwich Trench is important since it contributes to the studies of its tectonic history, which allows modelling of the subduction processes and deeper analysis of the compositions of fluxes from the subducting slab.

Data visualization

The complex analysis of the Scotia Sea basin and South Sandwich Trench is presented as a series of thematic maps prepared by the author (Figs 1–5), which help to summarized current data on tectonics, bathymetry, sediment thickness, marine free-air gravity anomalies and geoid, which are discussed below. Geomorphological plots are based on statistical computations using the GEBCO global topographic map of the seafloor features and geological and geophysical settings. The characteristics of the ocean floor structure are visualized according to the gravitational anomalies, geological parameters, geoid model and topographic terrain (Figs 1–5). The elevations and rift anomalies caused by the formation of oceanic crust and tectonic movements are evident along the axis of the Scotia Arc, South Sandwich Trench and faults near the Antarctic Peninsula.

The general bathymetric/topographic map covering the study area of the Scotia Sea and the South Sandwich Trench (Fig. 1) is based on the high-resolution raster grid (15-arc second) of the General Bathymetric Chart of the Oceans (GEBCO), a bathymetric and topographic grid of the Earth (GEBCO Compilation Group, 2020): https://www.gebco.net/. The tectonic and geological setting (Fig. 2) are visualized based on the ETOPO1 grid (Amante and Eakins 2009). The resolution and accuracy of ETOPO1 (1 arc minute) is high, in contrast to the ETOPO5 (5 arc minute) gridded topography data, which are based on contour maps rather than original soundings and have large errors (Smith 1993). Previous regional detailed topological and bathymetric maps of

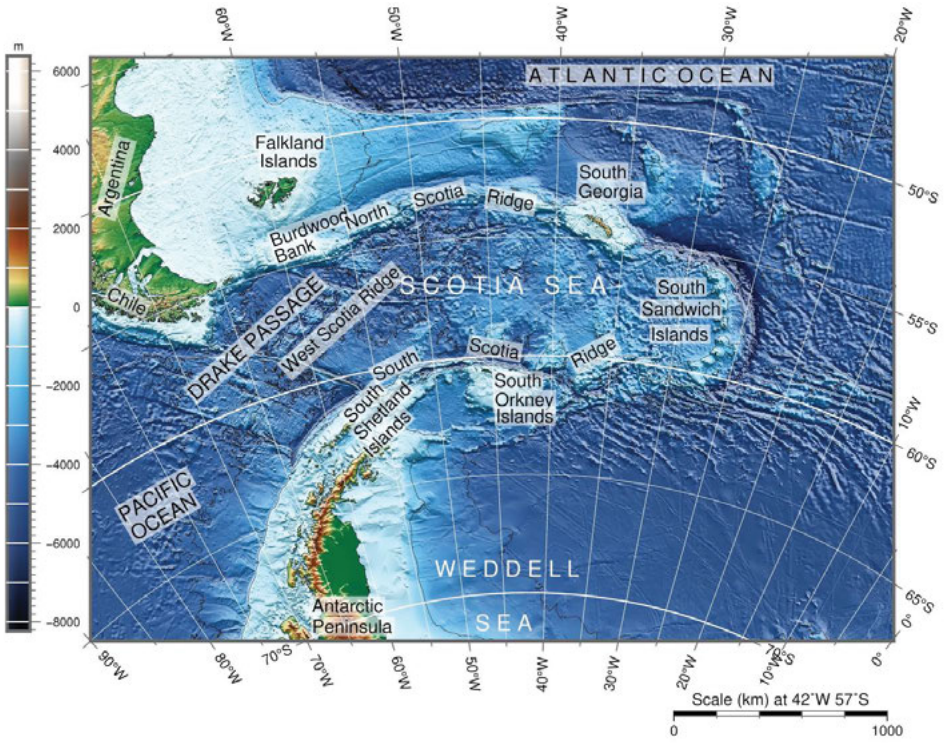

Fig. 1. Topographic map of the Scotia Sea region, prepared using GEBCO global terrain model, 15 arc second resolution grid (GEBCO Compilation Group 2020); Lambert Azimuthal Equal-Area projection, central meridian 42°W, standard parallel 57°S.

the Scotia Sea region (Leat *et al.* 2016) demonstrated that South Sandwich Islands are entirely volcanic in origin, and most have been volcanically active in historic times. A geopotential model of the Earth's gravity fields EGM96 was used as a base raster dataset for modelling the geoid data (Fig. 4) of the Scotia Sea and South Sandwich Trench (Lemoine *et al.* 1998). The free-air gravity data (Fig. 5) of the study area was derived from the satellite-derived free-air gravity grid (Sandwell and Smith 1997; Sandwell *et al.* 2014). The visualization of the global satellite-derived geoid or gravity anomaly data reveals the characteristics of the seamounts and seafloor fabric for analysis of their tectonic setting reflected in the relief by some sensitive parameters, *e.g.* elastic thickness of the lithosphere (Watts *et al.* 2006), and highlights the relations among the distributions of depth, seafloor area and age (Smith and Sandwell 1997). Sediment thickness was mapped from the raster global grid GlobSed, which is based on seismic reflection data (Straume *et al.* 2019). Earthquake focal mechanisms, represented as first-motion 'beach balls' (Fig. 2), were plotted using data from the global CMT project (Ekström *et al.* 2012).

Geographic location and topography

The Scotia Sea is located in the southern part of the Atlantic Ocean, close to the Antarctic, with coordinates in the ranges 53°S – 63°S, 25°W – 65°W (Fig. 1). The geographic borders of the Scotia Sea are the Drake Passage in the west and the Scotia Arc to the north, east, and south. The Scotia Arc is one of the Earth's most important ocean gateways and former land bridges (Maldonado *et al.* 2014), now forming the spatial borders of the Scotia Sea: North Scotia Ridge as the northern margin, the South Sandwich Islands as the east margin, and the South Scotia Ridge on the south (Barker 2001), and the East Scotia Ridge as the back-arc spreading center (Leat et al. 2000). The formation of the Scotia Arc developed as a result of the evolution of the Andean–West Antarctic Cordillera, which included its bending, disruption, and fragmentation in the Cenozoic (Dalziel and Elliot 1971).

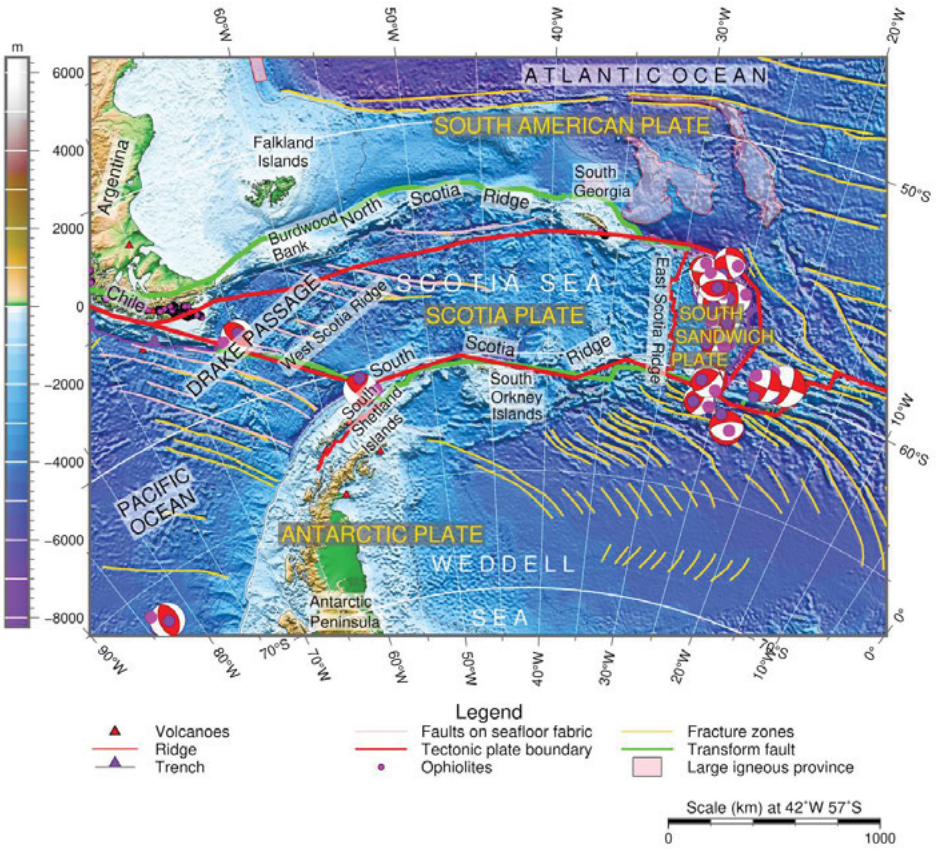

Fig. 2. Geologic setting of the Scotia Sea region, prepared using ETOPO1 global terrain model, 1 arc min resolution grid (Amante and Eakin 2009); Lambert Azimuthal Equal-Area projection, central meridian 42°W, standard parallel 57°S. The geologic features (faults earthquakes, tectonic plates) based on Bird (2003), Matthews *et al.* (2011), Seton *et al.* (2014) and Wessel *et al.* (2015).

The crescent of the Scotia Arc includes several minor islands and the South Sandwich Trench, located parallel to and east of the island arc. In general, there is an almost complete correlation between modern topographic relief of the seafloor in the Scotia Sea and its crystalline basement. At the tops of the elevated blocks of the South Scotia Ridge, the basement is partially exposed or covered by a layer of sediments exceeding 1 km (Maldonado *et al.* 2003). In general, the depths in Scotia Sea bathymetry do not exceed 4–5 km with occasional depths up to 6 km below sea level (bsl) in narrow channels and canyons extending along the foot of the Scotia Arc.

Geology and tectonic setting

The Scotia Sea is located on two minor tectonic plates, the Sandwich and Scotia plates. The Scotia Plate, located between the South American Plate and Antarctic Plate, was formed at about 30 to 6 Ma as a result of seafloor spreading on the West Scotia Ridge (Eagles *et al.* 2005; Riley *et al.* 2019), when spreading was active and ceased with activity at the junction with the North Scotia Ridge (Livermore *et al.* 2005), and older fragments of largely unknown age in the Central Scotia Sea, generally consistent with Mesozoic (Eagles 2010), see Fig. 2. The NE-SW oriented western Scotia Sea spreading centers included the southernmost South America and the Antarctic Peninsula inter-plate motion in late Paleogene and Neogene between 30 and 9 Ma (Cunningham *et al.* 1995).

The movement of the Phoenix Plate (also known as the Aluk Plate) in ~15 Ma was accommodated at an axis of divergence in the region of Drake Passage (Eagles 2003, 2004). Located east of the spreading axis in the SE Pacific Ocean, the Phoenix Plate was partially subducted beneath the Antarctic Peninsula (Janik *et al.* 2014). Starting from the end of the Miocene, this spreading axis ceased to accommodate plate divergence (Litvin 1980). As a result of these complex movements, the Scotia Plate was partially preserved in the modern Scotia Sea (Barker and Burrell 1977).

Origin of the Sandwich Plate

During the last stages of the tectonic evolution of this region, the Scotia and Sandwich plates experienced motions relative to South America and Antarctica. As a result, the Scotia Sea region presents a complex set of marginal basins bordered by a seismic belt of South American and Antarctic plates (Forsyth 1975; Thomas *et al.* 2003). Currently, the Scotia Sea evolves under the strong influence of the movement of three plates: South American, Antarctic and the smaller Scotia tectonic plate affecting the Scotia Sea region (Barker 1970; Eagles and Jokat 2014). Over 75% of the oceanic crust of the Scotia Sea is identified as being less

than 30 Myr old, formed almost entirely within this period as a complication of the South American-Antarctic plate boundary (Hill and Barker 1980).

Since the Scotia Sea belongs to the marginal sea basins, its seafloor formed at the East and West Scotia ridges is composed of basalt, but there are also pieces of other crust on the banks. Although the magmatism along the East Scotia Ridge is chemically heterogeneous (Fretzdorff *et al.* 2003), there is a common composition similar to the mid-ocean ridge basalt (MORB) component, typical for the most of the lavas from the East Scotia back-arc spreading center, aqueous fluids from altered MORB, and samples from the slab-influenced segments showing addition of a sediment melt (Fretzdorff *et al.* 2002). The variations in magma chemistry result from mantle processes, and include generation of silicic magmas in a dominantly basaltic environment. The rock composition of the selected volcanoes ranges from mafic to silicic and tholeiitic to calc-alkaline (Leat *et al.* 2003).

The South Sandwich volcanic arc erupts low-K tholeiitic rocks, covered by unexotic pelagic and volcanogenic sediments on the down-going slab (Tonarini *et al.* 2011). Besides, the comparison of the volcanic fluids in spatially distinct areas of the South Sandwich Islands arc shown variations in their chemical content: the northern volcanoes have a source of fluids originated from the oceanic crust, whereas southern volcanoes indicate a higher proportion of sediment-derived fluids, which proves that the sediment-derived fluids contribute to the regional magmatism while sediment-derived melt does not (Barry *et al.* 2006). The formation of the modern geomorphological structure of the modern relief began in the Eocene (Ewing *et al.* 1971). Therefore, the average speeds of vertical tectonic movements since the Neogene can be estimated at 0.12–0.15 mm/year (Smalley *et al.* 2007).

The tectonic movements in the South Sandwich Island volcanic arc, a classic intra-oceanic arc located on a young oceanic crust (Larter *et al.* 1998), resulted in the formation of thrust and reverse faults in the subduction zone (Barker and Griffiths 1972; De Wit 1977). The formation of the South Scotia Sea and South Scotia Ridge resulted from the crustal extension in the Late Paleocene to the Early Eocene (55 Ma) along with rift basin formation in the Fuegan Andes, caused by the separation of the South American and Antarctic continents (Dalziel *et al.* 2013). The formation of the Wadati–Benioff seismic zone and South Sandwich Trench resulted from the subduction of the southernmost segment of the South American Plate beneath the small South Sandwich Plate. Specifically, the high level of activity at the South Sandwich Trench reflects the rapid motion of the Sandwich Plate, which overrides the subducting slab of South American lithosphere (Livermore 2003).

Seafloor spreading rates vary in different parts of the Scotia Sea basin: the South Sandwich forearc, the North Scotia Ridge, the South Scotia Ridge, the South Shetland Islands Block and the Shackleton Fracture Zone. Thus, the continental crust of the South Shetland Islands is about 10 to 12 km thick near the

slope, and becomes more than 15 km thick to the south while Ona High, to the norther of South Shetland Islands, has a variation of maximum thickness of 10 km to the slightly thicker than 6 km in the western, but highly thinned by faults (Maldonado *et al.* 2014). Its western part is covered by a thinner oceanic crust (6–8 km) caused by the depositional wedge, which consists of a thin volcanic layer with seismic velocities of 3.7–4.9 km/s and a basalt layer of 6.0–6.8 km/s. An upper mantle layer with a seismic velocity of *ca.* 8.2 km/s is located below (Litvin 1987). Geophysical analyses show that basalt layers generally differ from sedimentary layers by their more stable seismic velocity profiles, which demonstrates spatial variations in the tectonic settings of the studied areas. In the continent-ocean transition zones, it can be assumed that the basalt layer initially had a heterogeneous structure, similar to the granite-metamorphic layer, which was then gradually transformed in course of the geological development by significant basaltic intrusions that finally led to present-day homogeneity in rock constitution.

Sedimentation

The sediment thickness variation over the Scotia Sea (Fig. 3) is the result of its complexity of tectonic and geological settings, oceanographic regime, and submarine geomorphology, and is also tectonically affected by local subduction, erosion in a small area near the trench and strain regime (Cunningham *et al.* 1998; Vanneste and Larter 2002).

The GlobSed grid used in this study has been developed from previously published maps (Divins and Rabinowitz 1990; Divins 2003; Whittaker *et al.* 2013) and new data using mathematical formula for sediment thickness as a function of age and latitude that describes the sediment thickness pattern in the oceans (Straume *et al.* 2019). Variations in sediment thickness of the Scotia Sea shows that in the eastern part it is mostly about 1 km, while in its marginal depressions along the foot of the Scotia Arc it reaches up to 2–3 km. In contrast, in the western part of the Scotia Sea, sediment thickness is noticeably less, and in the area of ridges and channels of the Drake Passage, it intermittently and drastically decreases until absent (dark blue colors on Fig. 3), which may refer to the Drake Passage as one of the geochemical gateways of the Pacific Ocean (Pearce *et al.* 2001).

The greatest thickness of the sediment layer is notable on the areas placed close the Antarctic shelf: more than 4.5 km (orange to red colors on Fig. 3) followed by medium values of 3.5 to 4.5 km (cyan to light green colors on Fig. 3). Significant sediment thickness is observed on the downthrown blocks of the Scotia Arc. For example, the northern region around the South Orkney Islands is situated on a rise in the basement surface, while the area to the south is depressed and covered by marine sediments with a thickness of up to 2 km (Fig. 3).

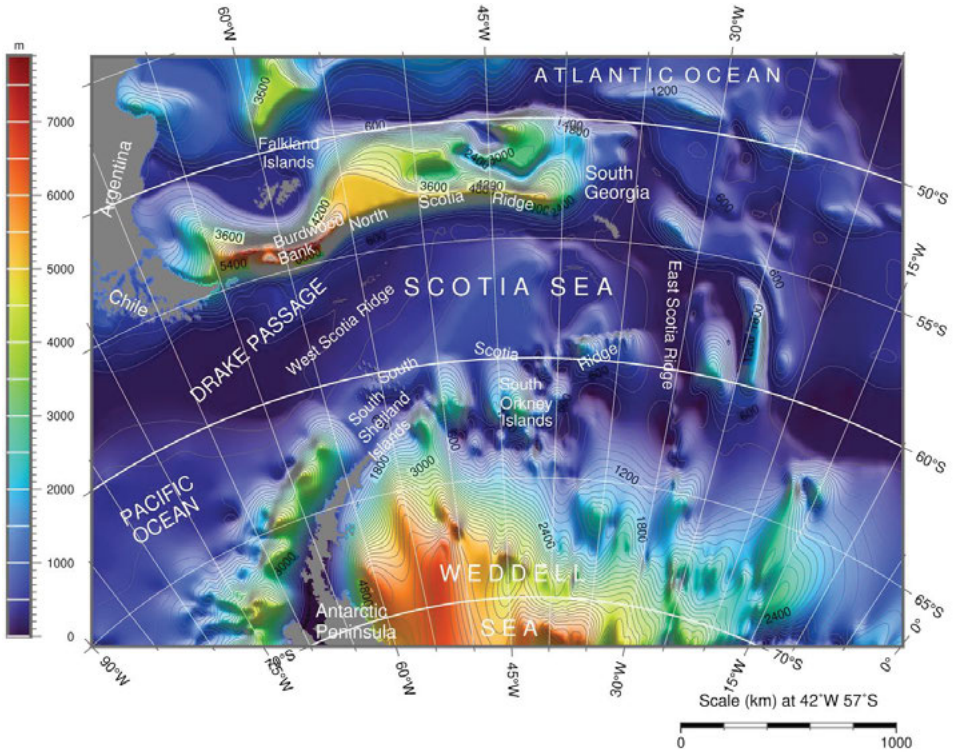

Fig. 3. Sediment thickness of the Scotia Sea seafloor, prepared using GlobSed 5 arc minute grid version 3 (Straume *et al.* 2019); Lambert Azimuthal Equal-Area projection, central meridian 42°W, standard parallel 57°S.

On the contrary, on the Burdwood Bank, a part of the North Scotia Ridge, the southern area is elevated while the northern parts are buried (Macfadyen 1933) beneath sediments whose thickness reaches up to 6.0 km.

Geomorphology

The geometry of the Scotia Sea in plan resembles a huge loop formed by the Scotia Arc. Its northern and southern sub-latitudinal branches are dominated by block structures. The arcuate form of the South Sandwich Trench and South Sandwich Islands is closely comparable to the Mariana Trench, as described in previous studies (Lemenkova 2019a). The constituent ridges are divided into a number of blocks, such as Burdwood Bank and the South Georgia, South Orkney and South Shetland Islands. These geomorphological blocks are punctuated mostly by the saddle depressions with depths of 2.5 to 3.0 km bsl, along the lines of oblique and transverse faults. The South Sandwich Islands are located *ca.* 100 km westward of the South Sandwich Trench, which exceeds

8000 m in depth and is associated with a Wadati–Benioff seismic zone (Thomas *et al.* 2003). The analysis of marine geophysical data in the Scotia Sea revealed a ridge crest-trench collision zone SE of the South Orkney Islands in the form of a double ridge with dissecting trough, oriented in a NE-SW direction (Barker *et al.* 1984). The dynamics in the Scotia Sea evolution can be explained by a series of such collision zones along the South Scotia Ridge, with some parts of the zone interpreted as remnant of the arc and upper fore-arc of an intra-oceanic arc produced by subduction of the South American Plate.

The geomorphological variety of the Scotia Sea indicates strong correlation of modern seafloor relief with the relief of the crystalline basement reflected by bathymetric geological and geophysical data (Beniest and Schellart 2020). Thus, the eastern part of the sea is notable for its arc-shaped banks and South Sandwich Trench, while its middle part is sculptured by a series of block rises. Channels and ridges dominate its western part. The eastern part of the Scotia Sea seafloor is dominated by submeridional submarine landforms. These include seafloor ridges of sediments at the margins of deep submarine canyon (elevations 500 to 1300 m), located to the western side of the South Sandwich Islands arc. The seafloor of the western part of the Scotia Sea is presented by a hilly plain with depths of about 4.0 km bsl. Along the eastern part of the Scotia Sea, there is an area of relatively low rifts, ridges and transverse deep channels stretching in NE direction (Barker and Hill 1981). Here, the South Sandwich arc lies on crust that formed at the back-arc spreading center, so older back-arc crust forms the basement of the present inner forearc (Larter 2003). In contrast, the regionally bathymetry of the central Scotia Sea is flat and shallow, characterized by relatively flat abyssal plain, which can be interpreted by an age over 80 Ma (Stein and Stein 1992). The maximum depth of the South Sandwich Sea is 8.239 m bsl located in South Sandwich Trench, according to the GEBCO dataset (15 arc sec resolution grid) used in this study.

Gravity anomalies based on EGM-2008 and WGS84 datum

The Scotia Sea is notable for its gravitational field anomalies, which are caused by a complex combination of geological structures and crustal types, as well as a significant marine and terrestrial geomorphological variability, in particular the stark contrast between mountainous coastlines and deep-sea trenches along the foot of the continental slope. The basin of the Scotia Sea is characterized by slightly positive or negative satellite derived free-air gravity approximation (Fig. 5). In general, one can see that positive relief forms, *i.e.* island arcs, ridges, rifts and minor elevations, correspond to moderate or intense positive free-air anomalies in the gravitational field (*e.g.*, comparing Fig. 1 and Fig. 5).

Clear local gravity field variations are associated with the block structure of the geomorphological uplifts and local elevations. For example, free-air gravity

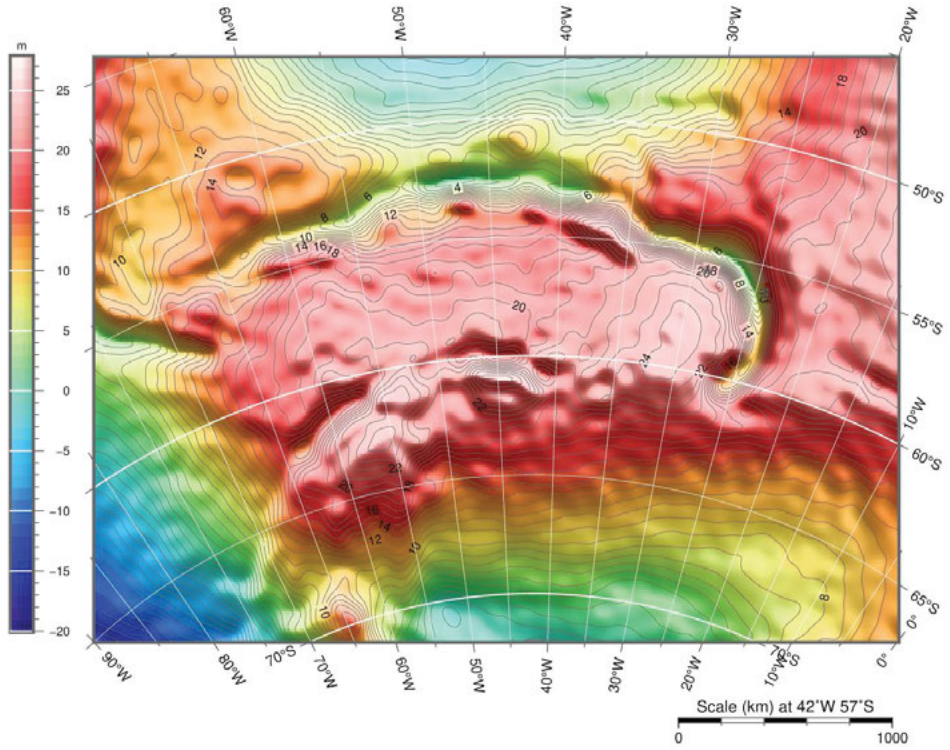

Fig. 4. Geoid gravitational regional model of the Scotia Sea basin, prepared using World geoid image 15 min resolution grid, version 9.2 EGM96 (Lemoine *et al.* 1998); Lambert Azimuthal Equal-Area projection, central meridian 42°W, standard parallel 57°S.

anomalies increase over the South Sandwich Islands, and decrease in the straits between them, which correspond to geomorphological depressions.

The correspondence of the gravity and topographic maps can be clearly seen by comparison of the bathymetric isolines on Fig. 1 and gravity values on Fig. 5. The South Sandwich Trench and submarine Scotia Ridge are characterized by significant large negative gravity anomalies (dark blue to almost black colors on Fig. 5). The eastern part of the Scotia Sea is dominated by free-air anomalies varying from 20 to 40 mGal (orange to to dark red colors on Fig. 5).

The Antarctic Peninsula shows a noticeable increase to 80 mGal. In the areas over the South Sandwich Island arc and local submarine elevations, the free-air anomalies range around 50 mGal and above, but over the north-eastern border of the volcanic South Sandwich Islands they exceed 80 mGal (light rose colors on Fig. 5). According to previous studies (Litvin 1987), Bouguer anomalies in the eastern part of the Scotia Sea range from 250 to 300, in the Drake Strait they reach up to 360, and over the South Sandwich Island areas they vary from 50 to 200 mGal. Further studies on the geophysical and geological setting of the Scotia Sea can be found in the relevant literature (*e.g.*, LaBrecque and

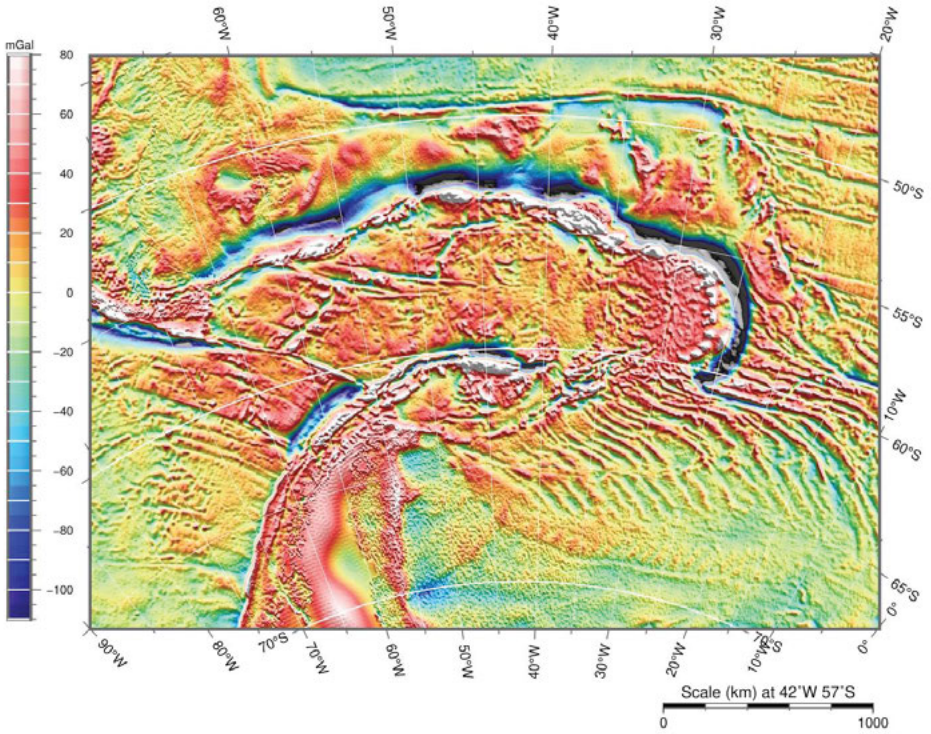

Fig. 5. Satellite derived free-air gravity approximation of the Scotia Sea basin, prepared using Global gravity grid from CryoSat-2 and Jason-1 (Sandwell *et al.* 2014); Lambert Azimuthal Equal-Area projection, central meridian 42°W, standard parallel 57°S.

Rabinowitz 1977; Ludwig and Rabinowitz 1982; Livermore *et al.* 1994; Pearce *et al.* 2000; Harrison *et al*. 2003; Leat *et al.* 2004, 2007; Eagles *et al.* 2006; Maldonado *et al.* 2013).

Bathymetry of the South Sandwich Trench

Scotia Sea is considered a special area because of its specific geodynamic, climate and circulation setting, as well as unique geographical location between the Drake Passage, south Pacific and Atlantic oceans, islands of South America, and the Antarctic Peninsula. The analysis of the study area indicates that bathymetry of the Scotia Sea varies in its different segments with diverse geologic and geodynamic setting that were formed in course of geologic evolution. The ultimate aim of this study was to track bathymetric variations in different segments of the South Sandwich Trench in a context of varied geodynamic conditions. To assess this heterogeneity, the GMT based methods for geospatial modeling were applied.

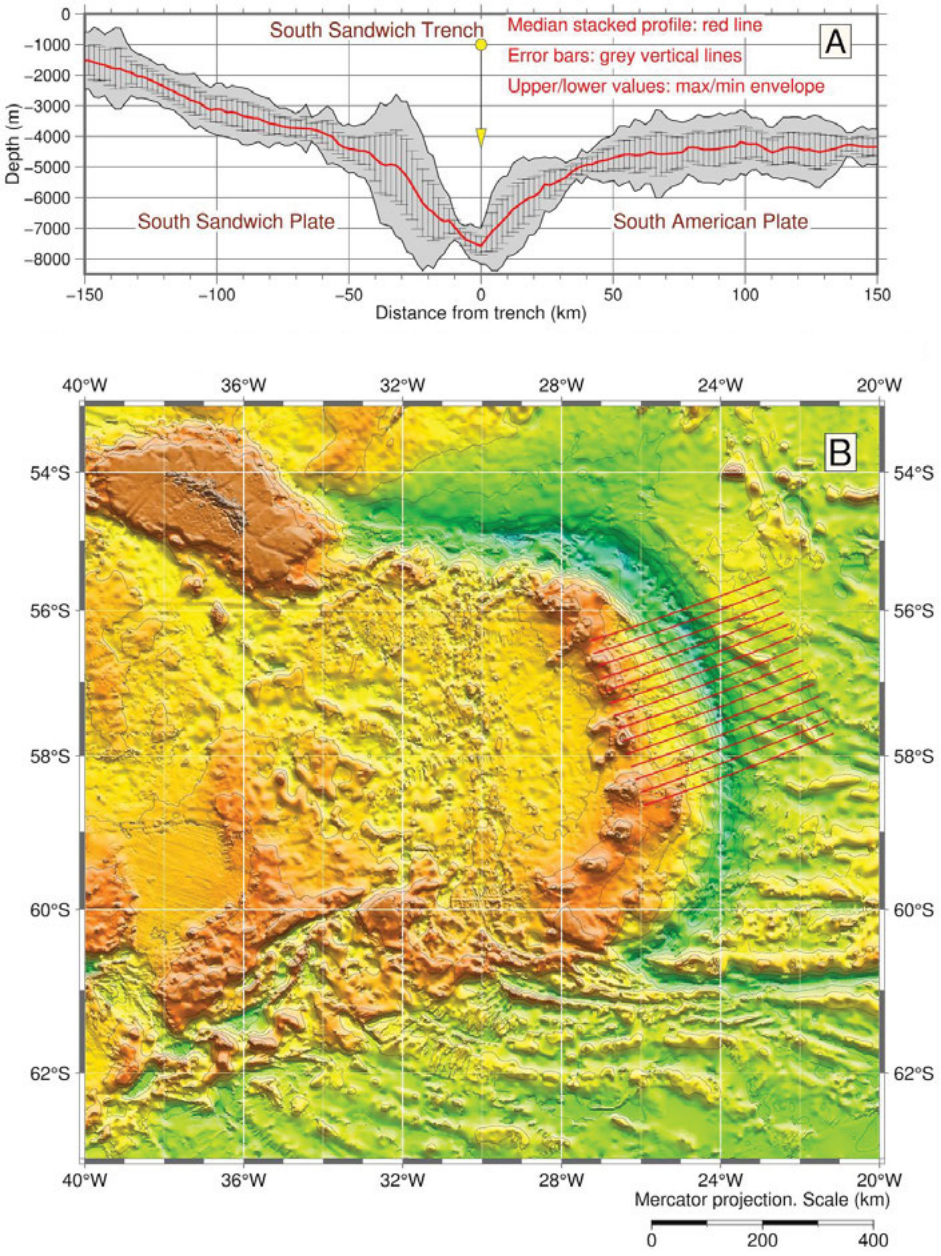

Fig. 6. Combined image of the South Sandwich Trench geomorphic cross-section profile (**A**) based on the GEBCO (GEBCO Compilation Group 2020), and their location (**B**). The red line in A means the median of the measured depths. The 14 thin red lines in B show the cross-section transects.

Methods. – The technical approach supporting the methodology of the current work is based on using the GMT, an open-source cartographic scripting toolset developed by American cartographers Paul Wessel and Walter Smith

(Wessel and Smith 1991) and continuously developed thereafter (Wessel *et al.* 2013; Wessel and Smith 2018). The cross-sectional profiles were digitized automatically with a spatial span of 300-km perpendicular to the trench axis, then plotted, visualized and statistically analyzed using tested algorithms of GMT syntax in shell scripts applied to this study (Lemenkova 2019b, 2019c, 2019d).

The geomorphological structure of the South Sandwich Trench was visualized as a series of 14 cross-sections (Fig. 6A) from a gridded bathymetric dataset (GEBCO 15 arc-second resolution). The 300-km-long cross sectional profiles were automatically digitized using a combination of the GMT modules 'grdtrack', 'gmtconvert' and 'psxy' and Unix auxiliary utilities ('cat', 'rm', 'echo') across the segments of the South Sandwich Trench across the line with coordinates 25.0°W, 56.0°S to 23.5°W, 58.2°S.

The 14 cross-section profiles, with a distance between each two of 20 km, sampled bathymetric depths every 2 km, along tracks perpendicular to the orientation of the South Sandwich Trench. The 14 cross-sections extend up to 150 km on either side of the trench (Fig. 6B) along a line drawn southwards along the most representative part of the trench (red line). The profiles were then visualized (Fig. 6A) from a table using the GMT module 'psxy'. The bathymetry of the South Sandwich Trench varies according to the recorded samples with each of the segments as shown on the statistical histogram (Fig. 7). From each cross-sectional profile, the statistics of the bathymetry of the South Sandwich Trench (minimum, maximum and median depths, and a standard deviation) was recorded and visualized over the topographic range of 8.239 to 0 km bsl (a completely submerged region with submarine topography) showing the

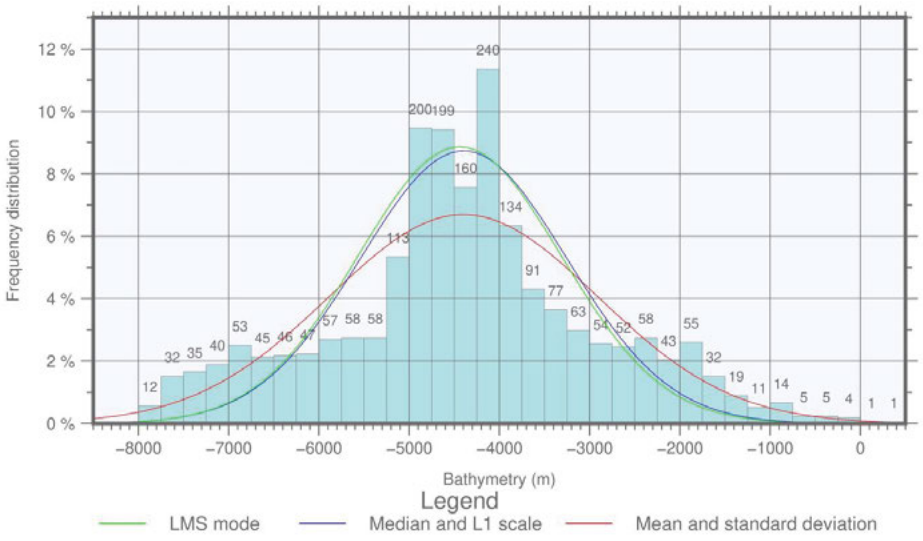

Fig. 7. Histogram of depths on the South Sandwich Trench geomorphology for the cross-section profiles from Fig. 6.

distribution of the geomorphological slopes by GMT modules 'pshistogram' and 'pslegend' (Fig. 7). The frequency of the data range, *i.e.* the repetitiveness of the depths, is visualized on Y-axis while the actual depths values are shown on the X-axis on Fig. 7.

Variations in morphological structure of the South Sandwich Trench. – Geomorphic structures of the Scotia Sea region are strongly correlated with marine free-air gravity anomalies. Fracture zones and transform faults of the West Scotia Ridge (Fig. 2), which form parallel to the direction of plate divergence, are interpretable in the marine free-air gravity anomalies (Fig. 5) based on the regional submarine topography (Fig. 1), dissecting the ridge and extending into flanking ocean basins. The distribution of the sediment thickness in the study area (Fig. 3) has higher values in the Falkland Islands and Antarctic shelf (Jokat and Herter 2016), dividing the Scotia Sea into regions with high sediment thickness (3 km and higher: green, yellow, orange and red colors on Fig. 3) and lower values (below the 3 km: blue colors on Fig. 3). This distribution correlates with the oceanographic regime of the Drake Passage and the Scotia Sea (Heywood and King 2002) as well as submarine geomorphological relief serving as a natural border, which correlates mainly with availability of continental sediment (compare Figs 1–3).

Besides, the oceanographic processes are major controlling factors for sediment distribution on the ocean floor in the Scotia Sea, because they determine the functionality and composition of plankton, as well as the influx of terrigenous material into the ocean. At the same time, bathymetry is a key factor for differentiating the distribution of various geologic types of the sediments, *e. g.*, clay, coarse, calcareous and others types of sediments. The geoid regional gravitation model (Fig. 4) demonstrates the shape of the Scotia Sea basin as a region with clearly distinct values above 13 m (bright red color on Fig. 4), while the Pacific Ocean (SW area) has gradually diminishing values of the geoid from 6 to -20: (light green, blue to dark blue colors on Fig. 4) with the most negative anomalies in the SW corner of the map, *i.e.*, the Bellingshausen Sea (Fig. 1). The geomorphology of the Scotia Sea is clearly depicted depressed curve corresponding to the actual relief of the Scotia Arc (compare Figs 1 and 4).

The series of 14 cross-sectional profiles is drawn perpendicular to the South Sandwich Trench reaching out to 150 km away from the center of the cross-sections plotted using methodology in the GMT. The error bars (Fig. 6A) show variations of the depths in each sample point, calculated as the statistical representations of the variability of the topographic data. Error bars are used on graph (Fig. 6A) to visualize uncertainty in the GEBCO dataset. The Scotia Plate and South American Plate are located on the western and eastern flanks of the trench, respectively. The maximum and minimum detected depths of the South Sandwich Trench are 8.239 m bsl (the deepest part of the axial valley) and 548 m bsl (the highest part of the western flank in the selected segment, Fig. 6A), respectively. Comparison is made between the parameters depicting the South

Sandwich Trench geomorphology, its 300 km-long cross-sectional topographic profiles, and its geological and geophysical features, such as marine free-air gravity and geoid heights variations, tectonics and sediment thickness.

The analysis of the topographic data frequency (Fig. 7) shows a classic bell--shaped histogram. The bell-shaped data distribution demonstrates a gradual distribution of data and gentle geomorphological slope shape. The analysis of the table containing bathymetry of the South Sandwich Trench shows the following statistical results (Fig. 7). The most frequent depth range (240 sample values) occurs at 4.000 to 4.200 m bsl following by similarly-frequent ranges of 4.500 to 4.750 m bsl: 199 and 200 repetitive samples, respectively. The interval of 4.250 to 4.500 m bsl includes 160 data samples. There are 134 data samples in the interval of 3.750 to 4.000 m bsl and 113 samples in the interval of 5.000 m to 5.250 m bsl. The remaining data demonstrate a gradual decrease in the sampling frequency. The western side of the trench has a slope of 44.11°, while the eastern segment is 42.5°.

The shallower parts of the slopes show (histogram for data distribution in Fig. 7) a decrease in frequency exception for the bins at 2.250 to 2.500 m bsl (58 samples) and 1.750 to 2.000 m bsl (55 samples). The western continental slope of the South Sandwich Trench shows an abrupt decrease in elevation from the South Sandwich Islands eastward (Fig. 6B), correlated with gradually decreasing depth frequency as shown on Fig. 7. The lowest frequency is typical for the deepest areas of the trench, reflecting the very localized geological setting, and impact of tectonic plate movements. The interval from 5.250 to 6.000 m bsl has an almost flat data distribution (58, 58 and 57 bins) over its three bins of 250 m width. Afterwards, the distribution of deeper values shows a gradual decrease with the exception of the interval of 6.750 to 7.000 m bsl (53 samples). Other values decrease gradually from 47 samples (interval of 6.000 to 6.250 m bsl) to 12 samples (7.750 m to 8.000 m bsl).

Relation between submarine geomorphology of the South Sandwich Trench and sediment thickness

The geomorphology and depth of the South Sandwich Trench is largely controlled by the degree of bending and depth of the oceanic plate before subduction, both depending on tectonic historical setting, *i.e.*, the age of the oceanic plate (Khain 2001). In turn, the age of the oceanic lithosphere affects the amount of sediments accumulated on the seafloor basement; in general, the older the plate and the higher the biogenic productivity, the thicker the sediment layer on the basement (Lisitsyn 1974). The sediment supply is in turn controlled by climate variations and glaciation in the land areas of Antarctic (Kuhn *et al.* 2006), denudation and weathering processes, as well as oceanic transport systems to the Scotia Sea and across the Antarctic shelf.

Sediment in the South Sandwich Trench reached thickness of only a couple of tens or hundreds of meters, leading to the preservation of tectonic morphology in bathymetry. In general, sedimentation in ocean basins tends to level out local topographic elevations creating a planar seafloor. However, the South Sandwich Trench presents well sculptured geomorphology in its landforms. The outer slope of the trench is shaped by bend-faulting and sediment influx, while its inner slope is mostly shaped by processes related to plate subduction. The difference in slope steepness (Fig. 7) can be explained by the erosive margins developed in a sediment starved trench during subduction erosion in a process of tectonic plate movement (Khain and Lomize 2005). More detailed study of the effects of subduction erosion on trench steepness was presented by Vanneste and Larter (2002). The morphology of the South Sandwich Trench is not leveled-out by the sediments with the roughness of the seafloor causing tectonic abrasion and erosion of material from the Antarctic and South American plates (Fig. 6A). This results in trench-parallel escarpments offsetting the seafloor over kilometers. Individual ridges dominating the trench inner slope at accretionary margins (Fig. 6B) are not presented in the erosive margins of the South Sandwich Trench.

Conclusions

The GMT is distinct by the fact that it enables both console-based scripting and map visualization in a single toolset. The combination of fine cartographic mapping and histogram visualization is a valuable feature of GMT when considering that geographic phenomena are spatially distributed and that thematic datasets should be processed by various approaches: mapping, overlay, cross-sectional plotting, statistical analysis, all of which are possible in GMT. This paper demonstrated the functionality of GMT as a fine cartographic toolset with a special application for a complex geographic analysis of the Scotia Sea and South Sandwich Trench. According to the analyses, the geomorphology of the trench has an asymmetric V-shape with maximum depth -8,239 m, according to the GEBCO dataset (15 arc sec resolution grid). Slope gradients across the trench are high, varying in both flanks: the western side has a 44.11° steepness, the eastern segment 42.5°. The trench was modeled by a series of 14 automatically-digitized cross-sectional profiles, drawn perpendicular to the South Sandwich Trench, each with a length of 300 km, at 20 km separation and sampled every 2 km along the segment between coordinates 25.0°W, 56.0°S and 23.5°W, 58.2°S. The sea bottom depth distribution has a classic bell-shaped curve. The most frequent depths are in the interval 4 to 5 km below sea level. Other depths show a gradual decrease in frequency. The scarp of the submarine slope in the trench is semi-circular mimicking the shape of the South Sandwich Islands arc. Variations in the geomorphology of the trench are caused by the tectonic activity and geological setting, interpretable from rock composition signals in gravitational field anomalies.

Acknowledgements. – I am indebted to Philip Leat from British Antarctic Survey, Tomasz Janik from the Institute of Geophysics, Polish Academy of Sciences and two anonymous reviewers for their careful reading, critical reviews and constructive comments that helped improve both the maps and the text in an initial version of the typescript. The research has been implemented in the framework of the Project No. 0144--2019-0011, Schmidt Institute of Physics of the Earth, Russian Academy of Sciences.

References

AGTERBERG F.P. 1964. Statistical techniques for geological data. *Tectonophysics* 1: 233–255.

AMANTE C. and Eakins B.W. 2009. ETOPO1 1 Arc-Minute Global Relief Model: Procedures, Data Sources and Analysis. *NOAA Technical Memorandu*: 19.

BARKER P.F. 1970. Plate tectonics of the Scotia Sea region. *Nature* 228: 1293–1296.

BARKER P.F. 2001. Scotia Sea regional tectonic evolution: implications for mantle flow and palaeocirculation. *Earth-Science Reviews* 55: 1–39.

BARKER P.F. and BURRELL J. 1977. The opening of Drake passage. *Marine Geology* 25: 15–34.

BARKER P.F. and GRIFFITHS D.H. 1972. The evolution of the Scotia Ridge and the Scotia Sea. *Philosophical Transactions of the Royal Society London, Series A* 271: 151–183.

BARKER P.F. and HILL I.A. 1981. Back-arc extension in the Scotia Sea. *Philosophical Transactions of the Royal Society London, Series A* 300: 249–262.

BARKER P.F., BARBER P.L. and KING E.C. 1984. An early Miocene ridge crest-trench collision on the South Scotia Ridge near 36°W. *Tectonophysics* 102: 315–332.

BARRY T.L., PEARCE J.A., LEAT P.T., MILLAR I.L. and LE ROEX A.P. 2006. Hf isotope evidence for selective mobility of high-field-strength elements in a subduction setting: South Sandwich Islands. *Earth and Planetary Science Letters* 252: 223–244.

BENIEST A. and SCHELLART W.P. 2020. A geological map of the Scotia Sea area constrained by bathymetry, geological data, geophysical data and seismic tomography models from the deep mantle. *Earth-Science Reviews* 210: 103391.

BIRD P. 2003. An updated digital model of plate boundaries. *Geochemistry, Geophysics, Geosystems* 4: 1027.

CUNNINGHAM W.D., DALZIEL I.W.D., LEE T.-Y. and LAWVER L.A. 1995. Southernmost South America-Antarctic Peninsula relative plate motions since 84 Ma: implications for the tectonic evolution of the Scotia Arc region. *Journal of Geophysical Research* 100: 8257–8266.

CUNNINGHAM A.P., BARKER P.F. and TOMLINSON J.S. 1998. Tectonics and sedimentary environment of the North Scotia Ridge region revealed by side-scan sonar. *Journal of the Geological Society London* 155: 941–956.

DAHLIN T., SVENSSON M. and LINDH P. 1999. DC Resistivity and SASW for validation of effeiciency in soil stabilisation prior to road construction. *Procs. EEGS'99*.

DALZIEL I.W.D. and ELLIOT D.H. 1971. Evolution of the Scotia Arc. *Nature* 233: 246–251.

DALZIEL I.W.D., LAWVER L.A., NORTON I.O. and GAHAGAN L.M. 2013. The Scotia Arc: Genesis, Evolution, Global Significance. *Annual Review of Earth and Planetary Sciences* 41: 767–793.

DAVIS J.C. 1986. *Statistics and Data Analysis in Geology*. Wiley, New Jersey.

DE WIT M.J. 1977. The evolution of the Scotia Arc as a key to the reconstruction of southwestern Gondwanaland, *Tectonophysics* 37: 53–81.

DIVINS D.L. 2003. *Total Sediment Thickness of the World's Oceans and Marginal Seas.* NOAA National Geophysical Data Center, Boulder, CO.

DIVINS D.L. and RABINOWITZ P.D. 1990. Thickness of Sedimentary Cover for the South Atlantic. *In:* G.B. Udintsev (ed.) *International Geological-Geophysical Atlas of the Atlantic Ocean*. Intergovernmental Oceanographic Commission, Moscow: 126–127.

EAGLES G. 2003. Plate tectonics of the Antarctic – Phoenix plate system since 15 Ma. *Earth and Planetary Science Letters* 217: 97–109.

EAGLES G. 2004. Tectonic evolution of the Antarctic–Phoenix plate system since 15 Ma. *Earth and Planetary Science Letters* 217: 97–109.

EAGLES G. 2010. The age and origin of the central Scotia Sea. *Geophysical Journal International* 183: 587–600.

EAGLES G. and JOKAT W. 2014. Tectonic reconstructions for paleobathymetry in Drake Passage. *Tectonophysics* 611: 28–50.

EAGLES G., LIVERMORE R.A., FAIRHEAD J.D. and MORRIS P. 2005. Tectonic evolution of the west Scotia Sea. *Journal of Geophysical Research* 110: B02401.

EAGLES G., LIVERMORE R.A. and MORRIS P. 2006. Small basins in the Scotia Sea: the Eocene Drake Passage gateway. *Earth and Planetary Science Letters* 242: 343–353.

EKSTRÖM G., NETTLES M. and DZIEWONSKI A.M. 2012. The global CMT project 2004-2010: Centroid-moment tensors for 13,017 earthquakes. *Physics of the Earth and Planetary Interiors* 200–201: 1–9.

EWING J.I., LUDWIG W.J., EWING M. and EITTREIM S.L. 1971. Structure of the Scotia Sea and Falkland Plateau. *Journal of Geophysical Research* 76: 7118–7137.

FORSYTH D.W. 1975. Fault plane solutions and tectonics of the South Atlantic and Scotia Sea. *Journal of Geophysical Research* 80: 1429–1443.

FRETZDORFF S., LIVERMORE R.A., DEVEY C.W., LEAT P.T. and STOFFERS P. 2002. Petrogenesis of the back-arc East Scotia Ridge, South Atlantic Ocean. *Journal of Petrology* 43: 1435–1467.

FRETZDORFF S., HAASE K.M., LEAT P.T., LIVERMORE R A., GARBE-SCHÖNBERG C.-D., FIETZKE J. and STOFFERS P. 2003. ^{230}Th-^{238}U disequilibrium in East Scotia back-arc basalts: implications for slab contributions. *Geology* 31: 693–696.

GAUGER S., KUHN G., GOHL K., FEIGL T., LEMENKOVA P. and HILLENBRAND C. 2007. Swath-bathymetric mapping. *Reports on Polar and Marine Research* 557: 38–45.

GEBCO COMPILATION GROUP 2020. *GEBCO 2020 Grid*. DOI: 10.5285/a29c5465-b138-234d-e053-6c86abc040b9

GRAD M., GUTERCH A., JANIK T. and SRODA P. 2002. Seismic characteristic of the crust in the transition zone from the Pacific Ocean to the northern Antarctic Peninsula, West Antarctica. *Royal Society of New Zealand Bulletin* 35: 493–498.

HARRISON D., LEAT P.T., BURNARD P., TURNER G., FRETZDORFF S. and MILLAR I.L. 2003. Resolving mantle components in oceanic lavas from segment E2 of the East Scotia back-arc ridge, South Sandwich Islands. *In:* R.D. Larter and P.T. Leat (eds.) *Intra-Oceanic Subduction Systems: Tectonic and Magmatic Processes. Special Publication of the Geological Society of London* 219: 333–344.

HEYWOOD K.J. and KING B.A. 2002. Water masses and baroclinic transports in the South Atlantic and Southern oceans. *Journal of Marine Research* 60: 639–676.

HILL I.A. and BARKER P.F. 1980. Evidence for Miocene back-arc spreading in the central Scotia Sea. *Geophysical Journal of the Royal Astronomical Society* 63: 427–440.

JANIK T. 1997. Seismic crustal structure of the Bransfield Strait, West Antarctica. *Polish Polar Research* 18: 171–225.

JANIK T., GRAD M., GUTERCH A. and ŚRODA P. 2014. The deep seismic structure of the Earth's crust along the Antarctic Peninsula - A summary of the results from Polish geodynamical expeditions. *Global and Planetary Change Part B* 123: 213–222.

JOKAT W. and HERTER U. 2016. Jurassic failed rift system below the Filchner-Ronne-Shelf, Antarctica: New evidence from geophysical data. *Tectonophysics* 688: 65–83.

KHAIN V.E. 2001. *Tectonics of the continents and oceans*. Scientific world, Moscow (in Russian).

KHAIN V.E. and LOMIZE M.G. 2005. *Geotectonics with Fundamentals of Geodynamics: Textbook for Universities, 2nd Edition*. Knizhnyi dom Universitet, Moscow (in Russian).

KLAUČO M., GREGOROVÁ B., STANKOV U., MARKOVIĆ V. and LEMENKOVA P. 2013a. Determination of ecological significance based on geostatistical assessment: a case study from the Slovak Natura 2000 protected area. *Central European Journal of Geosciences* 5: 28–42.

KLAUČO M., GREGOROVÁ B., STANKOV U., MARKOVIĆ V. and LEMENKOVA P. 2013b. Interpretation of Landscape Values, Typology and Quality Using Methods of Spatial Metrics for Ecological Planning. *54th International Conference Environmental and Climate Technologies*. Riga, Latvia.

KLAUČO M., GREGOROVÁ B., STANKOV U., MARKOVIĆ V. and LEMENKOVA P. 2014. Landscape metrics as indicator for ecological significance: assessment of Sitno Natura 2000 sites, Slovakia, Ecology and Environmental Protection. *Proceedings of the International Conference*. March 19–20, 2014. Minsk, Belarus: 85–90.

KLAUČO M., GREGOROVÁ B., KOLEDA P., STANKOV U., MARKOVIĆ V. and LEMENKOVA P. 2017. Land planning as a support for sustainable development based on tourism: A case study of Slovak Rural Region. *Environmental Engineering and Management Journal* 2: 449–458.

KUHN G., HASS C., KOBER M., PETITAT M., FEIGL T., HILLENBRAND C.D., KRUGER S., FORWICK M., GAUGER S. and LEMENKOVA P. 2006. The response of quaternary climatic cycles in the South-East Pacific: development of the opal belt and dynamics behavior of the West Antarctic ice sheet. *Expeditionsprogramm Nr. 75 ANT XXIII/4, AWI Helmholtz Centre for Polar and Marine Research*.

LABRECQUE J.L. and RABINOWITZ P.D. 1977. *Magnetic anomalies bordering the continental margin of Argentina*, AAPG Map 826.

LARTER R.D., KING E.C., LEAT P.T., READING A.M., SMELLIE J. and SMYTHE D.K. 1998. South Sandwich Slices Reveal Much about Arc Structure, Geodynamics, and Composition. *Eos Transactions American Geophysical Union* 79: 281–281.

LARTER R.D., VANNESTE L.E., MORRIS P. and SMYTHE D.K. 2003. Structure and tectonic evolution of the South Sandwich arc. *Geological Society, London, Special Publications* 219: 255–284.

LEAT P.T., LIVERMORE R.A., MILLAR I.L. and PEARCE J.A. 2000. Magma supply in back-arc spreading center segment E2, East Scotia Ridge. *Journal of Petrology* 41: 845–866.

LEAT P.T., SMELLIE J.L, LARTER R.D. and MILLAR I.L. 2003. Magmatism in the South Sandwich arc. *In:* R.D. Larter and P.T. Leat (eds.) *Intra-Oceanic Subduction Systems: Tectonic and Magmatic Processes*. *Special Publication of the Geological Society of London* 219: 285–313.

LEAT P.T., PEARCE J.A., BARKER P.F., MILLAR I.L., BARRY T.L. and LARTER R.D. 2004. Magma genesis and mantle flow at a subducting slab edge: the South Sandwich arc-basin system. *Earth and Planetary Science Letters* 227: 17–35.

LEAT P.T., LARTER R.D. and MILLAR I.L. 2007. Silicic magmas of Protector Shoal, South Sandwich arc: indicators of generation of primitive continental crust in an island arc. *Geological Magazine* 144: 179–190.

LEAT P.T., TATE A.J., TAPPIN D.R., DAY S.J. and OWEN M.J. 2010. Growth and mass wasting of volcanic centers in the northern South Sandwich arc, revealed by new multibeam mapping. *Marine Geology* 275: 110–126.

LEAT P.T., DAY S.J., TATE A.J., MARTIN T.J., OWEN M.J. and TAPPIN D.R. 2013. Volcanic evolution of the South Sandwich volcanic arc, South Atlantic, from multibeam bathymetry. *Journal of Volcanology and Geothermal Research* 265: 60–77.

LEAT P., FRETWELL P., TATE A., LARTER R., MARTIN T., SMELLIE J., JOKAT W. and BOHRMANN G. 2016. Bathymetry and geological setting of the South Sandwich Islands volcanic arc. *Antarctic Science* 28: 293–303.

LEMENKOVA P. 2011. *Seagrass Mapping and Monitoring Along the Coasts of Crete, Greece*. M.Sc. Thesis. Netherlands: University of Twente.

LEMENKOVA P. 2019a. Statistical Analysis of the Mariana Trench Geomorphology Using R Programming Language. *Geodesy and Cartography* 45: 57–84.

LEMENKOVA P. 2019b. Topographic surface modelling using raster grid datasets by GMT: example of the Kuril-Kamchatka Trench, Pacific Ocean. *Reports on Geodesy and Geoinformatics* 108: 9–22.

LEMENKOVA P. 2019c. GMT Based Comparative Analysis and Geomorphological Mapping of the Kermadec and Tonga Trenches, Southwest Pacific Ocean. *Geographia Technica* 14: 39–48.

LEMENKOVA P. 2019d. Geomorphological modelling and mapping of the Peru-Chile Trench by GMT. *Polish Cartographical Review* 51: 181–194.

LEMENKOVA P. 2020a. GEBCO Gridded Bathymetric Datasets for Mapping Japan Trench Geomorphology by Means of GMT Scripting Toolset. *Geodesy and Cartography* 46: 98–112.

LEMENKOVA P. 2020b. Using GMT for 2D and 3D Modeling of the Ryukyu Trench Topography, Pacific Ocean. *Miscellanea Geographica* 25: 1–13.

LEMENKOVA P. 2020c. GMT Based Comparative Geomorphological Analysis of the Vityaz and Vanuatu Trenches, Fiji Basin. *Geodetski List* 74 1: 19–39.

LEMENKOVA P. 2020d. Fractal surfaces of synthetical DEM generated by GRASS GIS module r. surf.fractal from ETOPO1 raster grid. *Journal of Geodesy and Geoinformation* 7: 86–102.

LEMENKOVA P. 2020e. The geomorphology of the Makran Trench in the context of the geological and geophysical settings of the Arabian Sea. *Geology, Geophysics and Environment* 46: 205–222.

LEMENKOVA P., PROMPER C. and GLADE T. 2012. Economic Assessment of Landslide Risk for the Waidhofen a.d. Ybbs Region, Alpine Foreland, Lower Austria. Protecting Society through Improved Understanding. 11th International Symposium on Landslides and the 2nd North American Symposium on Landslides and Engineered Slopes (NASL), June 2–8, 2012. Banff, AB, Canada, 279–285.

LEMOINE F.G., KENYON S.C., FACTOR J.K., TRIMMER R.G., PAVLIS N.K., CHINN D.S., COX C.M., KLOSKO S.M., LUTHCKE S.B., TORRENCE M.H., WANG Y.M., WILLIAMSON R.G., PAVLIS E. C., RAPP R.H. and OLSON T.R. 1998. *NASA/TP-1998-206861: The Development of the Joint NASA GSFC and NIMA Geopotential Model EGM96*, Maryland, USA.

LINDH P. 2004. *Compaction- and strength properties of stabilised and unstabilised fine-grained tills*. PhD Thesis, Lund University, Lund.

LISITSYN A.P. 1974. *Sedimentation in the oceans. Quantitative distribution of sedimentary material*. Nauka, Moscow (in Russian).

LITVIN V.M. 1980. *Morphostructure of the bottom of the Atlantic Ocean and its development in the Mesozoic and Cenozoic*. Nauka, Moscow (in Russian).

LITVIN V.M. 1987. *Morphostructure of the ocean floor*. Nedra, Moscow (in Russian).

LIVERMORE R. 2003. Back-arc spreading and mantle flow in the East Scotia Sea. *Geological Society, London, Special Publications* 219: 315–331.

LIVERMORE R.A., MCADOO D. and MARKS K. 1994. Scotia Sea tectonics from high-resolution satellite gravity. *Earth and Planetary Science Letters* 123: 255–268.

LIVERMORE R.A., NANKIVELL A., EAGLES G. and MORRIS P. 2005. Paleogene opening of Drake Passage. *Earth and Planetary Science Letters* 236: 459–470.

LUDWIG W.J. and RABINOWITZ P.D. 1982. The collision complex of the North Scotia Ridge. *Journal of Geophysical Research* 87: 3731–3740.

MACFADYEN W.A. 1933. Fossil foraminifera from the Burdwood Bank and their geological significance. *Discovery Reports* 7: 1–16.

MALDONADO A., BARNOLAS A., BOHOYO F., GALINDO-ZALDÍVAR J., HERNÁNDEZ-MOLINA J., LOBO F., RODRÍGUEZ-FERNÁNDEZ J., SOMOZA L. and VÁZQUEZ J.T. 2003. Contourite deposits in the central Scotia Sea: the importance of the Antarctic Circumpolar Current and the Weddell Gyre flows. *Palaeogeography, Palaeoclimatology, Palaeoecology* 198: 187–221.

MALDONADO A., DALZIEL I. and LEAT P.T. 2013. Understanding the evolution of the Scotia arc. *EOS* 94: 272–272.

MALDONADO A., BOHOYO F., GALINDO-ZALDÍVAR J., HERNÁNDEZ-MOLINA F.J., LOBO F.J., LODOLO E., MARTOS Y.M., PÉREZ L.F., SCHREIDER A.A. and SOMOZA L. 2014. A model of oceanic development by ridge jumping: Opening of the Scotia Sea. *Global and Planetary Change* 123: 152–173.

MALDONADO A., DALZIEL I.W.D. and LEAT P.T. 2015. The global relevance of the Scotia Arc: An introduction. *Global and Planetary Change* 125: 1–8.

MATTHEWS K.J., MÜLLER R.D., WESSEL P. and WHITTAKER J.M. 2011. The tectonic fabric of the ocean basins. *Journal of Geophysical Research* 116: B12109.

OKOŃ J., GIŻEJEWSKI J. and JANIK T. 2016. New geological interpretation of multi-channel seismic profiles from the Pacific Margin of the Antarctic Peninsula. *Polish Polar Research* 37: 243–268.

PASHKEVICH I.K., RUSAKOV O.M., KUTAS R.I., GRYN D.N., STAROSTENKO V.I. and JANIK T. 2018. Lithospheric structure based on integrated analysis of geological-geophysical data along the DOBREfraction'99/DOBRE-2 profile (the East European Platform – the East Black Sea Basin). *Geofizicheskii Zhurnal (Geophysical Journal)* 40: 98–136.

PEARCE J.A., BARKER P.F., EDWARDS S.J., PARKINSON I.J. and LEAT P.T. 2000. Geochemistry and tectonic significance of peridotites from the South Sandwich arc-basin system, South Atlantic. *Contributions to Mineralogy and Petrology* 139: 36–53.

PEARCE J., LEAT P.T., BARKER P.F. and MILLAR I. 2001. Geochemical tracing of Pacific-to-Atlantic upper-mantle flow through the Drake Passage. *Nature* 410: 457–461.

RILEY T.R., CARTER A., LEAT P.T., BURTON-JOHNSON A., BASTIAS J., SPIKINGS R.A., TATE A.J. and BRISTOW C.S. 2019. Geochronology and geochemistry of the northern Scotia Sea: A revised interpretation of the North and West Scotia ridge junction. *Earth and Planetary Science Letters* 518: 136–147.

SANDWELL D.T. and SMITH W.H.F. 1997. Marine gravity anomaly from Geosat and ERS-1 satellite altimetry. *Journal of Geophysical Research. Solid Earth* 102: 10039–10054.

SANDWELL D.T., MÜLLER R.D., SMITH W.H.F., GARCIA E. and FRANCIS R. 2014. New global marine gravity model from CryoSat-2 and Jason-1 reveals buried tectonic structure. *Science* 346: 65–67.

SCHENKE H.W. and LEMENKOVA P. 2008. Zur Frage der Meeresboden-Kartographie: Die Nutzung von AutoTrace Digitizer für die Vektorisierung der Bathymetrischen Daten in der Petschora-See. *Hydrographische Nachrichten* 81: 16–21.

SETON, M., WHITTAKER J., WESSEL P., MÜLLER R.D., DEMETS C., MERKOURIEV S., CANDE S., GAINA C., EAGLES G., GRANOT R., STOCK J., WRIGHT N. and WILLIAMS S. 2014. Community infrastructure and repository for marine magnetic identifications. *Geochemistry, Geophysics, Geosystems* 5: 1629–1641.

SMALLEY JR., R., DALZIEL I.W.D., BEVIS M.G., KENDRICK E., STAMPS D.S., KING E.C., TAYLOR F.W., LAURIA E., ZAKRAJSEK A. and PARRA H. 2007. Scotia arc kinematics from GPS geodesy. *Geophysical Research Letters* 34: L21308.

SMITH W.H.F. 1993. On the accuracy of digital bathymetric data. *Journal of Geophysical Research* 98: 9591–9603.

SMITH W.H.F. and SANDWELL D.T. 1997. Global seafloor topography from satellite altimetry and ship depth soundings. *Science* 277: 1956–1962.

STEIN C. and STEIN S. 1992. A model for the global variation in oceanic depth and heat flow with lithospheric age. *Nature* 359: 123–128.

STRAUME E.O., GAINA C., MEDVEDEV S., HOCHMUTH K., GOHL K., WHITTAKER J.M., ABDUL FATTAH R., DOORNENBAL J.C. and HOPPER J.R. 2019. GlobSed: Updated total sediment thickness in the world's oceans. *Geochemistry, Geophysics, Geosystems* 20: 1756–1772.

SUETOVA I.A., USHAKOVA L.A. and LEMENKOVA P. 2005. Geoinformation mapping of the Barents and Pechora Seas. *Geography and Natural Resources* 4: 138–142.

THOMAS C., LIVERMORE R. and POLLITZ F. 2003. Motion of the Scotia Sea plates, *Geophysical Journal International* 155: 789–804.

TIIRA T., JANIK T., SKRZYNIK T., SKRZYNIK T., KOMMINAHO K., HEINONEN A., VEIKKOLAINEN T, VÄKEVÄ S. and KORJA A. 2020. Full-Scale Crustal Interpretation of Kokkola–Kymi (KOKKY) Seismic Profile, Fennoscandian Shield. *Pure and Applied Geophysics* 177: 3775–3795.

TONARINI S., LEEMAN W.P. and LEAT P.T. 2011. Subduction erosion of forearc mantle wedge implicated in the genesis of the South Sandwich Islands (SSI) arc: evidence from boron isotope systematics. *Earth and Planetary Science Letters* 301: 275–284.

VANNESTE L.E. and LARTER R.D. 2002. Sediment subduction, subduction erosion and strain regime in the northern South Sandwich forearc. *Journal of Geophysical Research* 107: B72149.

WATTS A.B., SANDWELL D.T., SMITH W.H.F. and WESSEL P. 2006. Global gravity, bathymetry and the distribution of submarine volcanism through space and time. *Journal of Geophysical Research* 111: B08408.

WESSEL P. and SMITH W.H.F. 1991. Free software helps map and display data. *Eos Transactions AGU* 72: 441.

WESSEL P. and SMITH W.H.F. 2018. *The Generic Mapping Tools. Version 4.5.18 Technical Reference and Cookbook*, Computer software manual. U.S.A.

WESSEL P., SMITH W.H F., SCHARROO R., LUIS J.F. and WOBBE F. 2013. Generic mapping tools: Improved version released. *Eos Transactions AGU* 94: 409–410.

WESSEL P., MATTHEWS K.J., MÜLLER R.D., MAZZONI A., WHITTAKER J.M., MYHILL R. and CHANDLER M.T. 2015. Semiautomatic fracture zone tracking, *Geochemistry, Geophysics, Geosystems* 16: 2462–2472.

WHITTAKER J., GONCHAROV A., WILLIAMS S., MÜLLER R.D. and LEITCHENKOV G. 2013. Global sediment thickness dataset updated for the Australian-Antarctic Southern Ocean. *Geochemistry, Geophysics, Geosystems* 14: 3297–3305.

YEGOROVA T., BAKHMUTOV V., JANIK T. and GRAD M. 2011. Joint geophysical and petrological models for the lithosphere structure of the Antarctic Peninsula continental margin. *Geophysical Journal International* 184: 90–110.

Received 31 August 2020
Accepted 4 January 2021